J|A|C|S ARTICLES

Published on Web 04/06/2009

Helical Transfer through Nonlocal Interactions

Xiaojian Wu,† Sunjun Ji,† Yi Li,† Baozong Li,† Xiulin Zhu,† Kenji Hanabusa,‡ and Yonggang Yang*,†

College of Chemistry, Chemical Engineering and Materials Science, Soochow University, Suzhou 215123, P.R. China, and Department of Functional Polymer Science, Faculty of Textile Science and Technology, Shinshu University, Ueda 386-8567, Japan

Received January 8, 2009; E-mail: ygyang@suda.edu.cn

Abstract: A pair of chiral bola-type enantiomers, LL-**12PyBr** and DD-**12PyBr**, was synthesized. They can cause physical gels in pure water. Sol−gel transcriptions were carried out to control mesoporous 1,4-phenylene−silica nanostructures and helicity using the organic self-assemblies of these amphiphiles as templates. Under acidic conditions, left-handed helical 1,4-phenylene−silica bundles were prepared using the self-assemblies of LL-**12PyBr** as templates. Additionally, right-handed helical silica and 1,4-phenylene−silica bundles were prepared using the self-assemblies of DD-**12PyBr** as templates. Under basic conditions, 1,4-phenylene−silica bundles were also obtained. However, it is hard to determine the handedness. For all of the 1,4-phenylene−silica bundles, it is interesting to find that the aromatic rings are packing in helix within the wall of the pore channels. Powder X-ray diffraction patterns indicated that the aromatic rings of 1,4-phenylene−silica bundles prepared under basic conditions showed a greater degree of order than those of 1,4-phenylene−silica bundles prepared under acidic conditions. Moreover, helical silica, 1,3-phenylene−silica, ethene−silica, and ethane−silica bundles were also prepared using the self-assemblies LL-**12PyBr** and DD-**12PyBr** as templates.

Introduction

Chiral and helical structures exist everywhere in Nature. Up to now, many efforts have been carried out to prepare chiral and helical nanomaterials. For example, helical carbon,[1] silicon carbide,[2] zinc oxide,[3] and silica[4] nanostructures have been prepared using physical methods. However, it is still hard to control the handedness. Single-handed helical and coiled silica nanotubes[5] and mesoporous silica nanofibers[6,7] have been prepared using the sol−gel transcription method, which are templated by the self-assemblies of chiral low-molecular weight amphiphiles. However, because the silicas are amorphous, the silicas should not be chiral on molecular scale. Therefore, they may be not suitable to be applied in chiral catalysis. In the field of hybrids, the periodic mesoporous materials with organic groups in the walls have attracted a lot of interest.[8−12] The organic groups can improve the dielectric constant and mechanical properties.[13] Therefore, this kind of materials could be applied in the fields of electronics, optoelectronics, and photonics. Moreover, since organic groups can offer opportunities for further modification, many kinds of functional materials can be prepared simply by modification. For the potential applications in chiral catalysis and separation, it is better to build chiral function groups in the walls of silica pore channels.

† Soochow University.
‡ Shinshu University.

(1) (a) Motojima, S.; Honshiya, S.; Hishikawa, Y. *Carbon* **2003**, *41*, 2658. (b) Qin, Y.; Zhang, Z.; Cui, Z. *Carbon* **2003**, *41*, 3072. (c) Qin, Y.; Zhang, Z.; Cui, Z. *Carbon* **2004**, *42*, 1917.
(2) Zhang, H.-F.; Wang, C.-M.; Wang, L.-S. *Nano Lett.* **2002**, *2*, 941.
(3) Kong, X. Y.; Wang, Z. L. *Nano Lett.* **2003**, *3*, 1625.
(4) Zhang, H.-F.; Wang, C.-M.; Buck, E. C.; Wang, L.-S. *Nano Lett.* **2003**, *3*, 577.
(5) (a) Jung, J. H.; Ono, Y.; Hanabusa, K.; Shinkai, S. *J. Am. Chem. Soc.* **2000**, *122*, 5008. (b) Jung, J. H.; Kobayashi, H.; Masuda, M.; Shimizu, T.; Shinkai, S. *J. Am. Chem. Soc.* **2001**, *123*, 8785. (c) Jung, J. H.; Ono, Y.; Shinkai, S *Chem.−Eur. J.* **2000**, *6*, 4552. (d) Seddon, A. M.; Patel, H. M.; Burkett, S. L.; Mann, S. *Angew. Chem., Int. Ed.* **2002**, *41*, 2988.
(6) (a) Yang, Y.; Suzuki, M.; Kimura, M.; Shirai, H.; Kurose, A.; Hanabusa, K. *Chem. Commun.* **2005**, 2032. (b) Yang, Y.; Suzuki, M.; Owa, S.; Shirai, H.; Hanabusa, K. *Chem. Commun.* **2005**, 4462. (c) Yang, Y.; Suzuki, M.; Owa, S.; Shirai, H.; Hanabusa, K. *J. Am. Chem. Soc.* **2007**, *129*, 581. (d) Wan, X.; Pei, X.; Zhao, H.; Chen, Y.; Guo, Y.; Li, B.; Hanabusa, K.; Yang, Y. *Nanotechnology* **2008**, *19*, 315602. (e) Chen, Y.; Guo, Y.; Zhao, H.; Bi, L; Pei, X; Li, B; Yang, Y. *Nanotechnology* **2008**, *19*, 355603. (f) Li, B.; Chen, Y.; Zhao, H.; Pei, X.; Bi, L.; Hanabusa, K.; Yang, Y. *Chem. Commun.* **2008**, 6366.
(7) Yang, Y.; Suzuki, M.; Fukui, H.; Shirai, H.; Hanabusa, K. *Chem. Mater.* **2006**, *18*, 1324.
(8) (a) Asefa, T.; MacLachlan, M. J.; Coombs, N.; Ozin, G. A. *Nature (London)* **1999**, *402*, 867. (b) Yoshina-Ishii, C.; Asefa, T.; Coombs, N.; MacLachlan, M. J.; Ozin, G. A. *Chem. Commun.* **1999**, 2539. (c) Asefa, T.; MacLachlan, M. J.; Grondey, H.; Coombs, N.; Ozin, G. A. *Angew. Chem., Int. Ed.* **2000**, *39*, 1808. (d) Asefa, T.; Kruk, M.; MacLachlan, M. J.; Coombs, N.; Grondey, H.; Jaroniec, M.; Ozin, G. A. *J. Am. Chem. Soc.* **2001**, *123*, 8520.
(9) (a) Inagaki, S.; Guan, S.; Fukushima, Y.; Ohsuna, T.; Terasaki, O. *J. Am. Chem. Soc.* **1999**, *121*, 9611. (b) Guan, S.; Inagaki, S.; Ohsuna, T.; Terasaki, O. *J. Am. Chem. Soc.* **2000**, *122*, 5660. (c) Kruk, M.; Jaroniec, M.; Guan, S.; Inagaki, S. *J. Phys. Chem. B* **2001**, *105*, 681–689.
(10) (a) Inagaki, S.; Guan, S.; Ohsuna, T.; Terasaki, O. *Nature (London)* **2002**, *416*, 304. (b) Yang, Q.; Kapoor, M. P.; Inagaki, S. *J. Am. Chem. Soc.* **2002**, *124*, 9694.
(11) (a) Lim, M. H.; Blanford, C. F.; Stein, A. *Chem. Mater.* **1998**, *10*, 467–470. (b) Melde, B. J.; Holland, B. T.; Blanford, C. F.; Stein, A. *Chem. Mater.* **1999**, *11*, 3302. (c) Stein, A.; Melde, B. J.; Schroden, R. C. *Adv. Mater.* **2000**, *12*, 1403.
(12) Sayari, A.; Hamoudi, S.; Yang, Y.; Moudrakovski, I. L.; Ripmeester, J. R. *Chem. Mater.* **2000**, *12*, 3857.
(13) Lu, Y.; Fan, H.; Doke, N.; Loy, D. A.; Assink, R. A.; LaVan, D. A.; Brinker, C. J. *J. Am. Chem. Soc.* **2000**, *122*, 5258.

10.1021/ja9001376 CCC: $40.75

Because it is difficult to design and synthesize chiral silsesquioxanes which are suitable to be used as hybrid silica precursors, it is still hard to prepare chiral mesoporous hybrid silicas.[14]

Organic−inorganic hybrid silicas have been widely studied.[15] Recently, several series of chiral silsesquioxanes were synthesized. These compounds can self-assemble into helical morphologies. After polycondensation, helical hybrid silica bundles were obtained.[16] Namely, the chirality of organic groups was transferred to hybrid silica bundles through hydrogen and covalent bondings. Because the hybrid silicas are chiral at molecular levels, they are suitable to be applied in chiral catalysis.[17] Recently, it was reported by us that left-handed helical 1,4-phenylene−silica nanotubes with helical packing aromatic rings were prepared using an anionic gelator and a costructure-directing agent.[18] However, the wide-angle X-ray diffraction pattern indicated that the aromatic rings are not packing in high-order. Herein, we successfully transferred the chirality of organic self-assemblies to the packing of aromatic rings within the wall of porous 1,4-phenylene−silica through nonlocal interactions under both acidic and basic conditions. It was found that the aromatic rings of the porous 1,4-phenylene−silicas prepared under basic conditions are packing in a greater degree of order than those of the porous 1,4-phenylene−silicas prepared under acidic conditions.

Experimental Section

General Methods. Circular dichrosim (CD) spectra were measured on an AVIV 410 spectrophotometer. The CD spectra of hybrid silicas were taken by using the suspensions in optical purity methanol. TEM images were obtained using a TecnaiG220. FESEM images were taken on a Hitachi S-4700. Specific surface area and pore-size distribution were determined by the Brunauer−Emmett−Teller (BET) and nonlocal density functional theory (NLDFT) methods using N_2 adsorption isotherm measured by a ASAP 2020M+C instrument. Wide-angle X-ray diffraction (WAXRD) and small angle X-ray diffraction (SAXRD) patterns were taken on an X'Pert-Pro MPD X-ray diffractometer.

1,2-Bis(triethoxysilyl)ethane (**3**) and 1,2-bis(triethoxysilyl)ethene (**4**) were purchased from Gelest. Tetraethyl orthosilicate (TEOS), 1,3-bis(triethoxysilyl)benzene (**5**), and 1,4-bis(triethoxysilyl)benzene (BTEB) were purchased from Aldrich. Pyridine was obtained from Wako. 6-Bromohexanoyl chloride was obtained from Alfa Aesar. ValC_{12}Val (**1**) was prepared by deprotection of the carbobenzyloxy group.[19]

Synthesis of Compound Dodecamethylene-1,12-bis(*N*-(6-bromohexanoyl)-L-valine) (2). To a dry THF (500 mL) solution of **1** (20 mmol) and triethylamine was slowly added 6-halohexanoyl chloride (50 mmol) at 0 °C for 1 h and an additional 5.0 h at room temperature; the resulting solution was evaporated to dryness. The ethanol solution was added to vigorously stirred water (3.0 L). The white precipitate was filtered, washed with water, and then dried. The product was obtained by recrystallization from ethanol−ether. FT-IR (KBr): 3286 cm^{-1} (ν_{N-H}, amide A), 1634 cm^{-1} ($\nu_{C=O}$, amide I), 1548 cm^{-1} (δ_{N-H}, amide II). ^{1}H NMR (400 MHz, DMSO-d_6, TMS, 25 °C): δ = 0.83−0.86 (m, 12H; CH_3), 1.24 (br, 16H; alkyl), 1.35−1.41 (m, 8H; $BrCH_2CH_2C\underline{H_2}\underline{CH_2}$), 1.51−1.58 (m, 4H; $CONHCH_2C\underline{H_2}$), 1.78−1.86 (m, 4H; $BrCH_2C\underline{H_2}$), 1.89−1.91 (m, 2H; $(CH_3)_2C\underline{H}$), 2.21−2.25 (m, 4H; $C\underline{H_2}CONH$), 2.97−3.15 (m, 4H; $CONHC\underline{H_2}$), 3.46 (t, J = 6.8 Hz, 4H; CH_2Br), 4.10−4.14 (m, 2H; N$\underline{H}$CHCO), 7.78 (t, J = 5.3 Hz, 2H; CON$\underline{H}CH_2$). $C_{34}H_{64}Br_2N_4O_4$ (M_w; 752.70). Elemental analysis calcd (%): C, 54.25; H, 8.57; N, 7.44. Found: C, 54.31; H, 8.88; N,7.45.

Synthesis of Compound Dodecamethylene-1,12-bis(*N*-(6-pyridiumhexanoyl)-L-valine)dibromide (LL-12PyBr). A pyridine solution (100 mL) of compound **2** (20 mmol) was heated at 100 °C for 12 h under a nitrogen atmosphere. The resulting solution was evaporated to dryness. The product was obtained by recrystallization twice from ethanol−ether (yield: 97%). FT-IR (KBr): 3285 cm^{-1} (ν_{N-H}, amide A), 1634 cm^{-1} ($\nu_{C=O}$, amide I), 1547 cm^{-1} (δ_{N-H}, amide II). ^{1}H NMR: (400 MHz, DMSO-d_6, TMS, 25 °C): δ = 0.79−0.81 (m, 12H; CH_3), 1.22 (br, 20H; alkyl), 1.35−1.38 (m, 4H; $NHCOCH_2C\underline{H_2}$), 1.50−1.57 (m, 4H; $CONHCH_2C\underline{H_2}$), 1.85−1.97 (m, 6H; $PyCH_2C\underline{H_2}$, $(CH_3)_2C\underline{H}$), 2.10−2.24 (m, 4H; $C\underline{H_2}CONH$), 2.91−3.13 (m, 4H; $CONHC\underline{H_2}$), 4.05−4.10 (m, 2H; NHC$\underline{H}$CO), 4.62 (t, J = 7.3 Hz, 4H; $PyC\underline{H_2}$), 7.78 (d, J = 8.8 Hz, 2H; CON$\underline{H}$CH), 7.91 (t, J = 5.6 Hz, 2H; CON$\underline{H}CH_2$), 8.17 (t, J = 6.6 Hz, 4H; 3-Py$\underline{H}$), 8.62 (t, J = 7.6 Hz, 2H; 4-Py$\underline{H}$), 9.13 (d, J = 8.8 Hz, 4H; 2-Py$\underline{H}$). $C_{44}H_{74}Br_2N_6O_4$ (M_w; 910.9). Elemental analysis calcd (%): C, 58.02; H, 8.19; N, 9.23. Found: C, 58.11; H, 8.43; N, 9.19.

Synthesis of Compound Dodecamethylene-1,12-bis(*N*-(6-pyridiumhexanoyl)-D-valine)dibromide (DD-12PyBr). FT-IR (KBr): 3285 cm^{-1} (ν_{N-H}, amide A), 1636 cm^{-1} ($\nu_{C=O}$, amide I), 1543 cm^{-1} (δ_{N-H}, amide II). ^{1}H NMR: (400 MHz, DMSO-d_6, TMS, 25 °C):δ = 0.78−0.81 (m, 12H; CH_3), 1.21 (br, 20H; alkyl), 1.35−1.37 (m, 4H; $NHCOCH_2C\underline{H_2}$), 1.50−1.58 (m, 4H; $CONHCH_2C\underline{H_2}$), 1.85−1.96 (m, 6H; $PyCH_2C\underline{H_2}$, $(CH_3)_2C\underline{H}$), 2.09−2.23 (m, 4H; $C\underline{H_2}CONH$), 2.89−3.12 (m, 4H; $CONHC\underline{H_2}$), 4.05−4.09 (m, 2H; NHC$\underline{H}$CO), 4.60 (t, J = 7.2 Hz, 4H; $PyC\underline{H_2}$), 7.83 (d, J = 8.8 Hz, 2H; CON$\underline{H}$CH), 7.96(t, J = 5 Hz, 2H; CON$\underline{H}CH_2$), 8.17 (t, J= 6.6 Hz, 4H; 3-Py$\underline{H}$), 8.62 (t, J = 7.8 Hz,2H; 4-Py$\underline{H}$), 9.12 (d, J = 6.4 Hz; 2-Py$\underline{H}$). $C_{44}H_{74}Br_2N_6O_4\cdot H_2O$ (M_w; 928.92). Elemental analysis calcd (%): C, 56.89; H, 8.25; N, 9.05. Found: C, 57.03; H, 9.01; N, 8.82.

Preparation of Multiple Helical 1,4-Phenylene−Silica Nanofibers under Acidic Conditions. A typical preparation process was shown as following. LL-**12PyBr** (100 mg, 0.11 mmol) was dissolved in 1.0 mL of 2.4 M HCl aq. to form a viscous solution, and then 100 mg (0.25 mmol) of precursor BTEB was dropped into the solution and strongly stirred at room temperature. After the reaction mixture turned white, stirring was stopped. The gel was kept at room temperature for 1 day and 80 °C for 4 days under static conditions. Finally, the gelator was removed by extracting with a mixture of 100 mL of methanol and 5.0 mL of 36.0 wt % HCl aqueous for 48 h, and then the obtained 1,4-phenylene−silica was dried in air.

Preparation of Multiple 1,4-Phenylene−Silica Nanofibers under Basic Conditions. A typical preparation process was shown as following. LL-**12PyBr** (50 mg, 0.055 mmol) was dissolved in 1.0 mL of 0.25 M NaOH aq. to form a viscous solution, and then 120 mg (0.30 mmol) of precursor BTEB was dropped into the solution and strongly stirred at room temperature. After the reaction mixture turned white, stirring was stopped. The gel was kept at room temperature for 1 day and 80 °C for 4 days under static conditions. Finally, the gelator was removed by extracting with a mixture of 100 mL of methanol and 5.0 mL of 36.0 wt % HCl aqueous for 48 h, and then the obtained 1,4-phenylene−silica was dried in air.

(14) MacQuarrie, S.; Thompson, M. P.; Blanc, A.; Mosey, N. J.; Lemieux, R. P.; Crudden, C. M. *J. Am. Chem. Soc.* **2008**, *130*, 14099.
(15) (a) Fujita, S.; Inagaki, S. *Chem. Mater.* **2008**, *20*, 891. (b) Yiu, H. H. P.; Wright, P. A. *J. Mater. Chem.* **2005**, *15*, 3690. (c) Hunks, W. J.; Ozin, G. A. *J. Mater. Chem.* **2005**, *15*, 3716. (d) Nakanishi, K.; Kanamori, K. *J. Mater. Chem.* **2005**, *15*, 3776. (e) Moreau, J. J. E.; Pichon, B. P.; Bied, C.; Wong Chi Man, M. *J. Mater. Chem.* **2005**, *15*, 3929.
(16) (a) Moreau, J. J. E.; Vellutini, L.; Wong Chi Man, M.; Bied, C. *J. Am. Chem. Soc.* **2001**, *123*, 1509. (b) Yang, Y.; Nakazawa, M.; Suzuki, M.; Kimura, M.; Shirai, H.; Hanabusa, K. *Chem. Mater.* **2004**, *16*, 3791. (c) Yang, Y.; Nakazawa, M.; Suzuki, M.; Shirai, H.; Hanabusa, K. *J. Mater. Chem.* **2007**, *17*, 2936.
(17) Kawasaki, T.; Ishikawa, K.; Sekibata, H.; Sato, I.; Soai, K. *Tetrahedron lett.* **2004**, *45*, 7939.
(18) Chen, Y.; Li, B.; Wu, X.; Zhu, X.; Suzuki, M.; Hanabusa, K.; Yang, Y. *Chem. Commun.* **2008**, 4948.
(19) Suzuki, M.; Owa, S.; Yumoto, M.; Kimura, M.; Shirai, H.; Hanabusa, K. *Tetrahedron Lett.* **2004**, *45*, 5399.

Scheme 1. Synthesis of Gelator LL-**12PyBr** and Molecular Structures of DD-**12PyBr** and Precursors

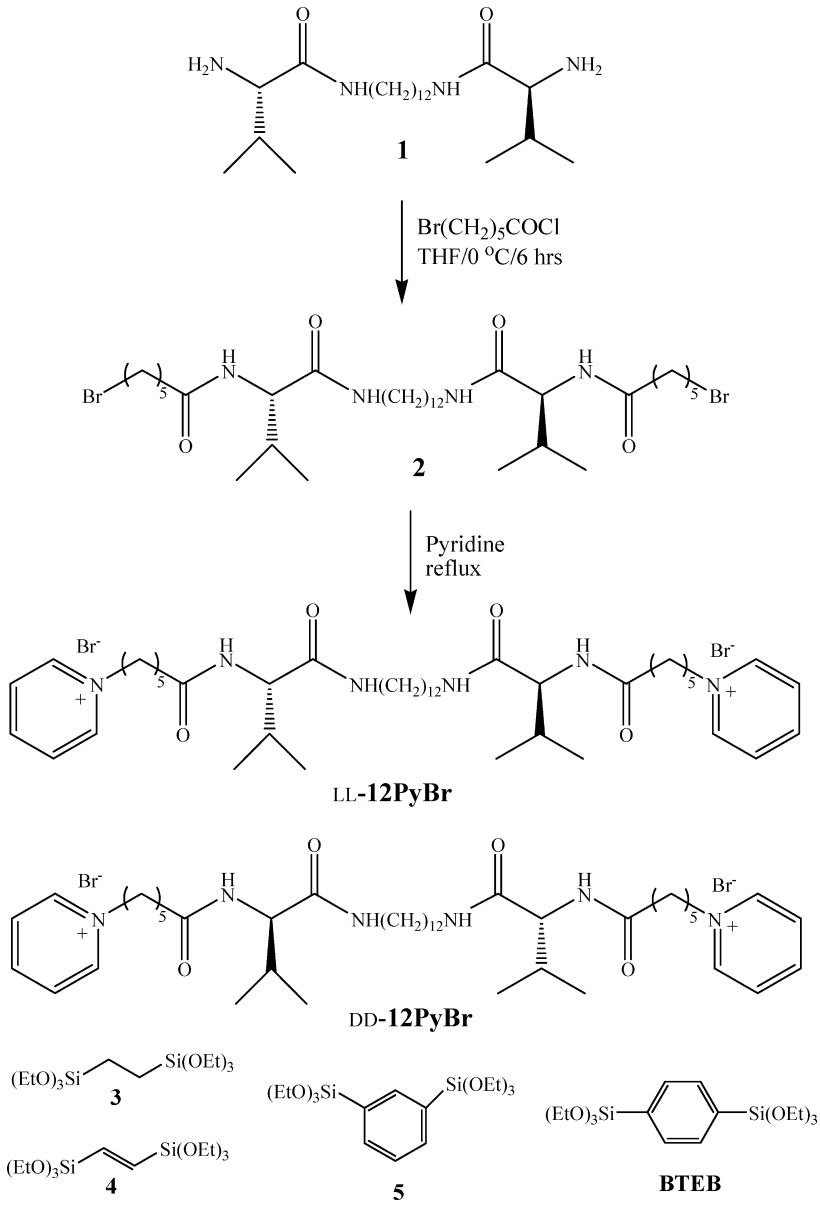

The preparation of silicas and other hybrid silicas is shown in Supporting Information.

Results and Discussion

Physical Properties of LL-12PyBr. The synthetic process of LL-**12PyBr** was shown in Scheme 1. The gelation properties of LL-**12PyBr** have been reported previously.[19] It can self-assemble into helical bundles in pure water.[6a] The CD and UV spectra of the LL-**12PyBr** and DD-**12PyBr** hydrogels are shown in Figure 1. Compound LL-**12PyBr** shows a negative CD sign at 200 nm. On the contrary, DD-**12PyBr** shows a positive CD sign at 200 nm. A UV absorption band originating from the pyridinium rings was identified at 259 nm. Because no clear induced CD signs were identified at 259 nm, there should be no strong $\pi-\pi$ interactions among the pyridinium rings.

Multiple Helical 1,4-Phenylene−Silica Nanofibers under Acidic Conditions. Left- and right-handed multiple helical 1,4-phenelene−silica nanofibers (LL-**PS** and DD-**PS**) were obtained using LL-**12PyBr** and DD-**12PyBr**, respectively (Figure 2). The obtained hybrid silica was a kind of cotton-like material and showed elasticity. The cotton-like fibers, which should be bundles of nanofibers, could be identified by the polarized optical micrograph and by the naked eye(Figure 2c and e), when they were suspended in methanol. FESEM images of the left-handed helical 1,4-phenylene−silica bundles are shown in Figure 2a, b, and c. These hybrid silica bundles were very well aligned (Figure 2a and b), although the overlap of the bundles occurred during the FESEM sample preparation process. The alignment of bundles occurred during the sol−gel transcription process. The shear force of stirring plays an important role on the alignment.[20] The alignment of nanofibers was systematically studied by varying the reaction conditions. The results indicate that a high concentration of the gelators more than 5.0 wt % is essential in the case of LL-**12PyBr**. At this concentration, the gelator LL-**12PyBr** formed stiff gel in 2.4 M HCl aq. at room temperature. It means that the packing of nanofibers in high density is essential for the alignment of nanofibers (Figure 2a).

(20) Yang, Y.; Suzuki, M.; Kimura, M.; Shirai, H.; Hanabusa, K. *Chem. Commun.* **2004**, 1332.

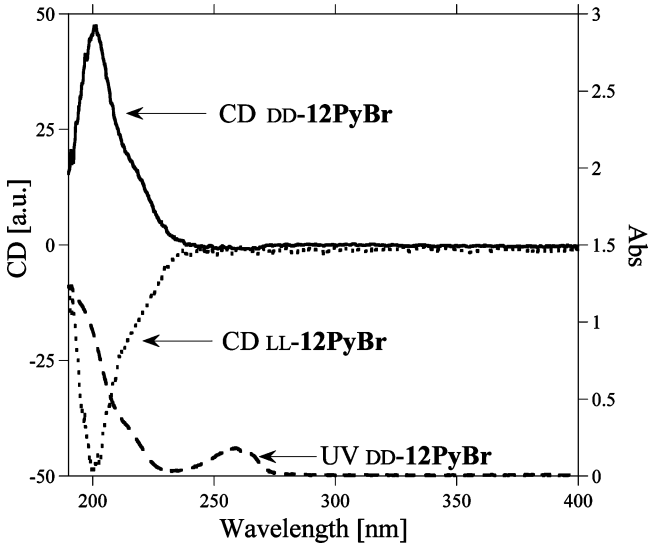

Figure 1. CD and UV spectra of LL-**12PyBr** and DD-**12PyBr** hydrogels.

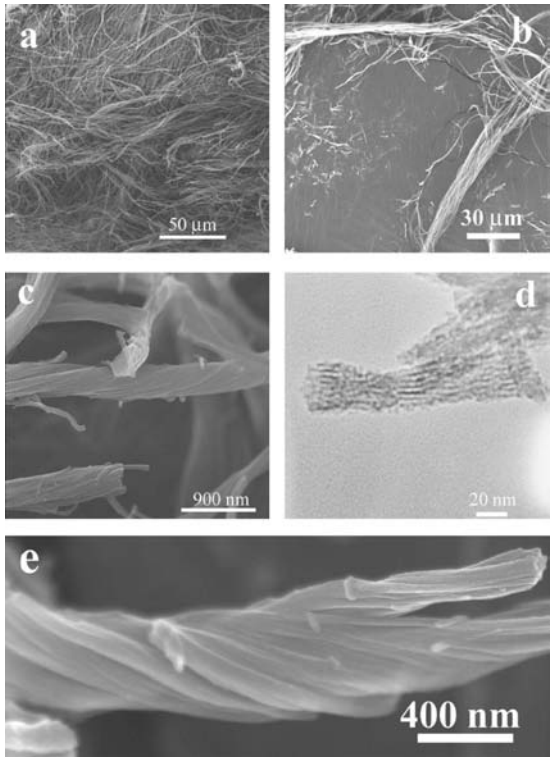

Figure 2. FESEM (a, b, and c) and TEM (d) images of left-handed multiple helical mesoporous 1,4-phenylene−silica nanofibers; FESEM image (e) of right-handed multiple helical mesoporous 1,4-phenylene−silica nanofibers.

The packing in high density will ensure the alignment of nanofibers being kept during the workup procedure. When the concentration of gelators is low, the fibers could not be aligned very well, and most of the fibers were randomly dispersed. With respect to stirring, high speed is essential not only for BTEB dissolving in HCl aq. but also for the alignment of nanofibers. Amorphous and randomly aligned hybrid fibers are obtained if the stirring is insufficient. The gelation property of LL-**12PyBr** is sensitive to pH; namely when the concentration of HCl is too high, gelator LL-**12PyBr** fails to form a gel. Therefore, the concentration of HCl can affect the morphologies; for instance, a stronger acid condition will result in an amorphous hybrid.

The diameters of the bundles ranged from 300 to 500 nm. The long-range order of nanofibers can reach 200 μm (Figure 2b), although the nanofibers may be broken during the SEM sample preparation process. Figure 2c shows the enlarged images of the hybrid silica bundles. It was found that each bundle was formed by many ultrafine nanofibers with a left-handed helical sense. The diameters of the ultrafine fibers were uniform at 40 nm. The pore channels of an ultrafine fiber were identified in the TEM image (Figure 2d). It seems that the ultrafine fibers are also helical.[21]

The nitrogen adsorption−desorption isotherm plot of LL-**PS** is shown in Figure 3a. Micropores, mesopores, and macropores exist in them. The micropores should be the void within the wall of pore channels, and the macropores should be the void among the bundles. The mesopores are the void templated by the self-assemblies of LL-**12PyBr**. Multiple helical hybrids were first prepared from self-templated monomers by Moreau's group in 2001.[16a] The surface area was around 100 m^2/g. In our study, the self-assemblies of gelators were used as the templates. Due to the formation of tubular structure after removing the template, the BET surface area reaches 571 m^2/g, which is larger than that of the self-directed structured hybrid fibers.[16] This material seems more suitable as the substrate of catalysts. Perhaps the most interesting thing is that the present hybrid material is not powder and shows elasticity. Namely, it is easily handled and removed from reaction mixtures. NLDFT pore-size distribution at the adsorption branch shows peaks at 1.0−3.0 nm. Mesoporous silica bundles prepared from LL-**12PyBr** under basic condition have been reported previously.[6a] The diameters of the pore channels are also around 2.0 nm.

The WAXRD pattern at medium diffraction angles shows two broad peaks at $d = 8.0$ and 4.0 Å (Figure 4a). The smallest repeat unit length of the 1,4-phenylene−silicas is around 8.0 Å. The distance between each two neighbor aromatic rings is around 4.0 Å. The aromatic rings did no packing at high-order degree,[18] even though it is also found that the aromatic rings are packing in helix within the walls of the pore channels. The CD spectrum of LL-**PS** shows two positive signs at 234 and 287 nm. Although LL-**PS**s are left-handed helical bundles, the first induced CD sign originating from the benzene rings is positive which seems to indicate that the aromatic rings are packing in right-handed.[22] Handedness inversion has been revealed in many systems. For example, a right-handed helical protein chain can pack into a left-handed helical superstructure.[23] The handedness of organic self-assemblies is sensitive to solvents and temperature.[6e] Right-handed helical polymer chains can organize into left-handed superhelical structures.[24] Handedness inversion has also been shown in the self-directed association of chiral molecules in bridged silsesquioxanes due to linker length.[25] Therefore, although LL-**12PyBr** packs in left-handed, the obtained secondary structure on a nanolevel may be right-handed. Moreover, this right-handed helical sense was transferred to the benzene rings of 1,4-phenylene−silicas through

(21) Che, S.; Liu, Z.; Ohsuna, T.; Sakamoto, K.; Terasaki, O.; Tatsumi, T. *Nature (London)* **2004**, *429*, 281.
(22) Autschbach, J.; Ziegler, T.; van Gisbergen, S. J. A.; Baerends, E. J. *J. Chem. Phys.* **2002**, *116*, 6930.
(23) Malashkevich, V. N.; Kammerer, R. A.; Efimov, V. P.; Schulthess, T.; Engel, J. *Science* **1996**, *274*, 761.
(24) Cornelissen, J. J. L. M.; Fischer, M.; Sommerdijk, N. A. J. M.; Nolte, R. J. M. *Science* **1998**, *280*, 1427.
(25) Xu, Q.; Moreau, J. J. E.; Vellutini, L.; Wong Chi Man, M. *J. Sol.-Gel Sci. Technol.* **2004**, *32*, 111.

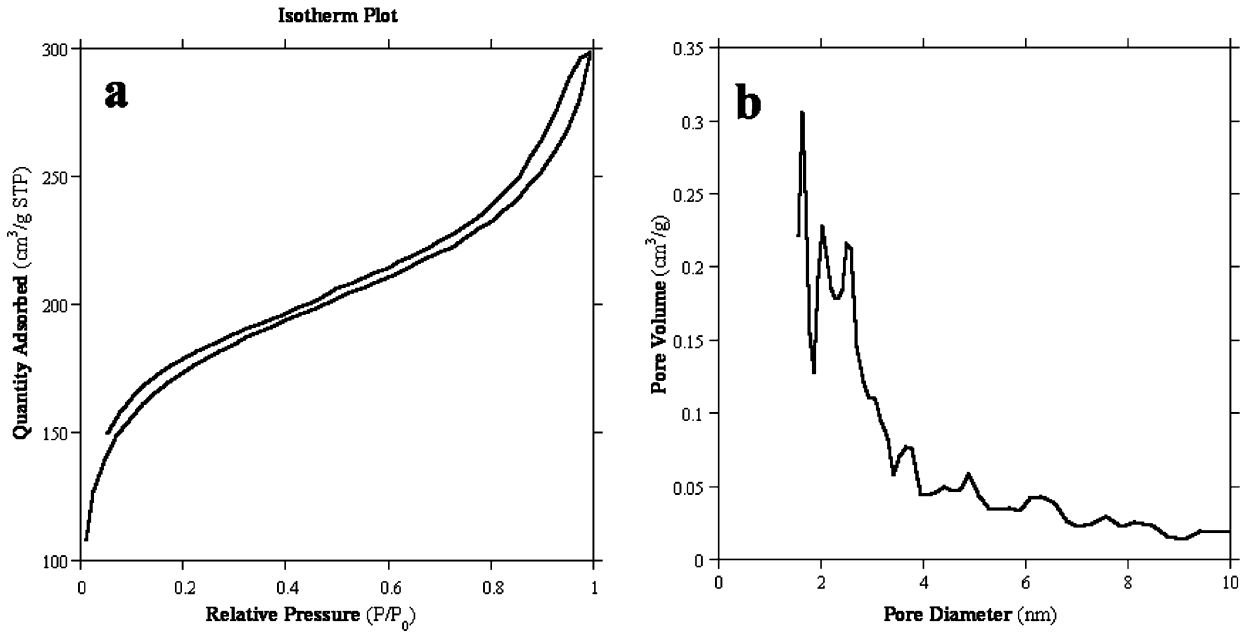

Figure 3. Nitrogen adsorption−desorption isotherm plot (a) and NLDFT pore-size distribution at adsorption branch (b) of left-handed helical hybrid silica bundles.

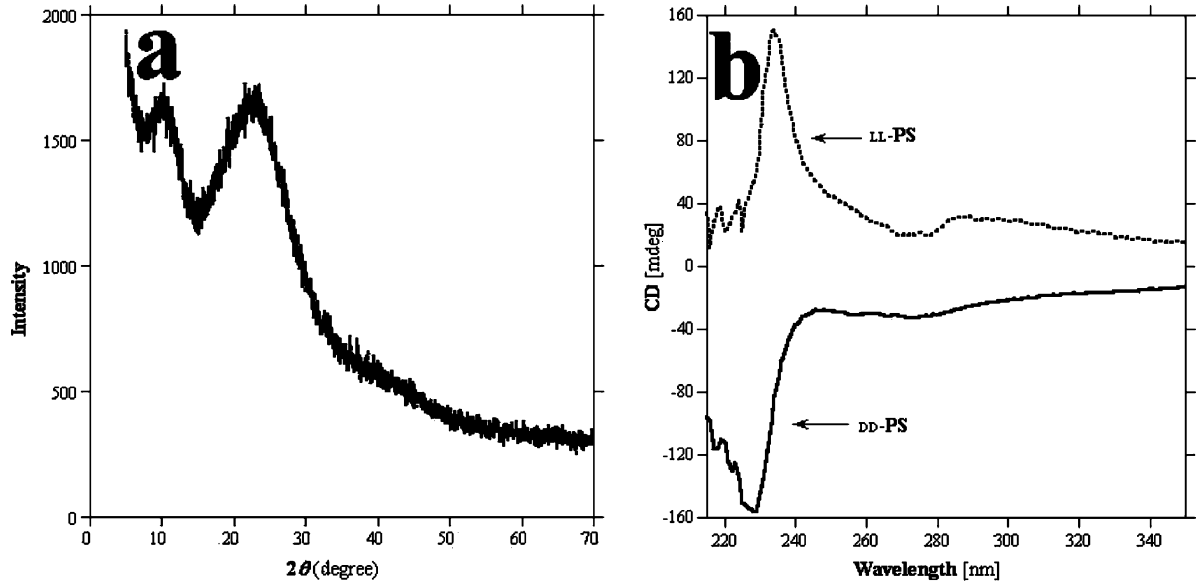

Figure 4. WAXRD pattern (a) of LL-**PS** and CD spectra (b) of LL-**PS** and DD-**PS**.

nonlocal interactions. The CD spectrum of DD-**PS** shows one strong negative sign at 229 nm.

This material shows high thermally stability. It turned just to yellow even when it was heated at 500 °C for 10 h under air. The temperature for decomposition is around 540 °C under nitrogen (Supporting Information, Figure S1). The stability is probably brought about by the $\pi-\pi$ stacking between phenylene segments in the walls of the tubes.[10] Therefore, we had to calcine the hybrids at 650 °C for 5 h under air to remove organic segments. It is very interesting to note that the morphologies were kept, even after removing phenylene segments by calcination (Figure 5). The helical bundles were kept, even being calcined at 1000 °C for 2.0 h under air. However, the mesopores disappeared (Supporting Information, Figure S2). When they were calcined at 1000 °C for 3.0 h under argon, although few

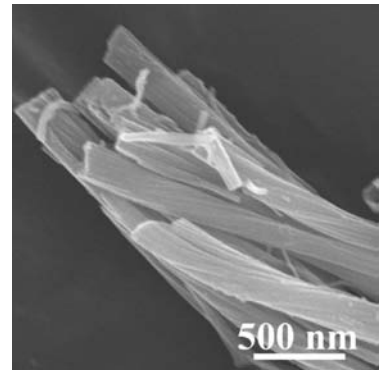

Figure 5. Calcined LL-**PS** bundles.

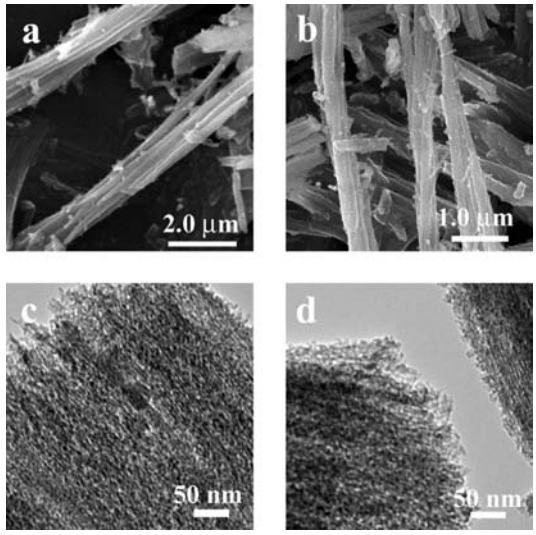

Figure 6. FESEM (a) image of the LL-**PS** prepared under basic conditions; FESEM (b) and TEM (c and d) images of the DD-**PS** prepared under basic conditions.

helical bundles were identified, most of them melted (Supporting Information, Figure S3).

Up to now, many efforts were carried out to illustrate the formation of helical structures. For example, entropy[26,27] and surface free energy[28] are supposed as the driving force of the helix formation. Moreover, the handedness of organic aggregates is sensitive to stirring directions.[29] Single-handed helical mesoporous silica fibers were prepared by controlling stirring directions and speed.[30] Although vortex force can affect the handedness of organic aggregates, it did not play an important role on controlling the handedness of the hybrid silica bundles shown here. Under the same stirring direction and speed, left-handed helical LL-**PS** bundles and right-handed helical DD-**PS** ones were obtained using the self-assembled LL-**12PyBr** and DD-**12PyBr**, respectively. When the stirring speed was decreased, left-handed helical bundles combined with some hybrid silica nanoballs were prepared from LL-**12PyBr**, which should be formed due to the deficient stirring (Supporting Information, Figure S4). Very recently, it was reported that capillary force can induce nanobristles to self-organize into helical clusters.[31] However, for the hybrid silicas shown here, the handedness of organic self-assemblies should be the main driving force for the formation of helical bundles,[5a] because LL-**12PyBr** can self-organize into single-handed helical bundles in solvents under static conditions.[6a] If these helical bundles are driven by the capillary force, both left- and right-handed helical bundles should be obtained. However, only single-handed helical bundles were obtained (Figure 2 and Figure S4, Supporting Information). Recently, the mechanism of the formation of single-handed helical mesoporous structures has been illustrated using TEM at different reaction times.[6d,f] These indicated that helical structures had already formed in the reaction mixtures. The organic amphiphiles reorganized into helical morphologies during the sol−gel transcription process. The chirality of the organic self-assemblies was transferred to the ultrafine nanofibers, then to the bundles.

Multiple 1,4-Phenylene−Silica Nanofibers under Basic Conditions. Inagaki's results indicated that the benzene rings can be well organized under basic conditions.[10] Herein, we carried out a sol−gel transcription process using NaOH as catalyst. However, the concentration of NaOH should be less than 2.0 N, because the gelators would precipitate out at that concentration. Therefore, the sol−gel transcription reactions were carried out in 0.25 N NaOH aq. solutions. FESEM and TEM images of the LL-**PS** and DD-**PS** bundles are shown in Figure 6. Most of them are straight (Figure 6a), and only a few of them show somewhat helical sense (Figure 6b). The morphologies of the hybrid silicas are sensitive to reaction conditions. This phenomenon was also found in other systems.[16a,32] Under acidic or weak basic conditions, the chiral templates tended to reorganize into helical morphologies during the sol−gel transcription process.[6d16a], However, under stronger basic conditions, the hydrolysis and polycondensation of silica sources are faster than the reorganization of templates. Although the chiral templates tended to form helical morphologies, perfect helical silica and hybrid silica nanostructures could not be

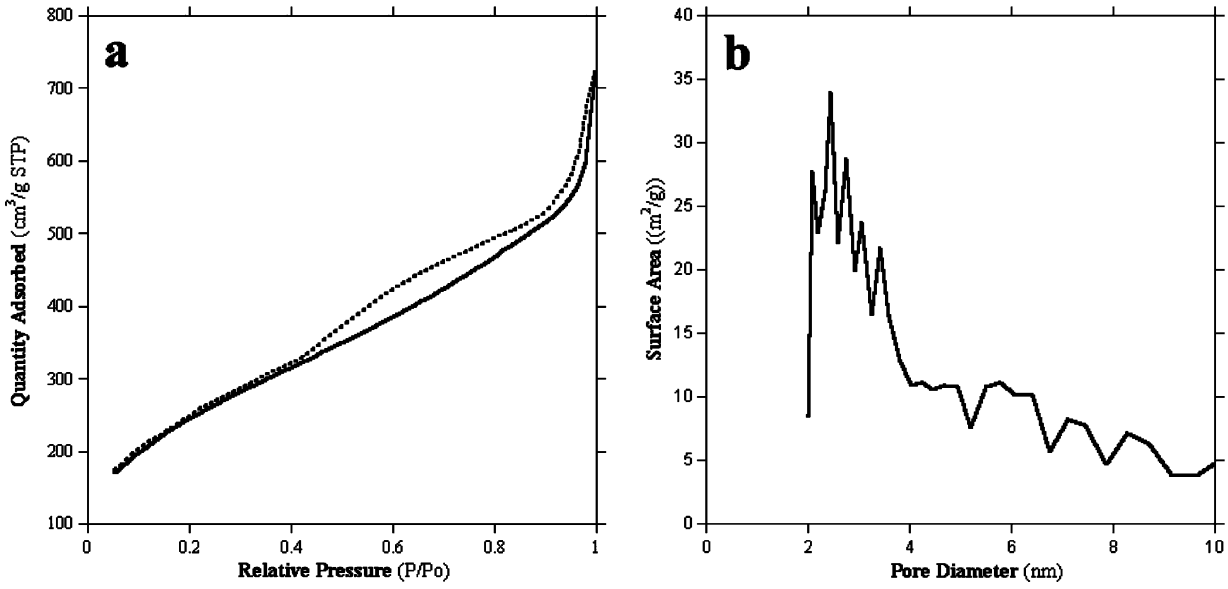

Figure 7. The nitrogen adsorption−desorption isotherm plot (a) and NLDFT pore-size distribution at adsorption branch (b) of the LL-**PS** prepared under basic conditions.

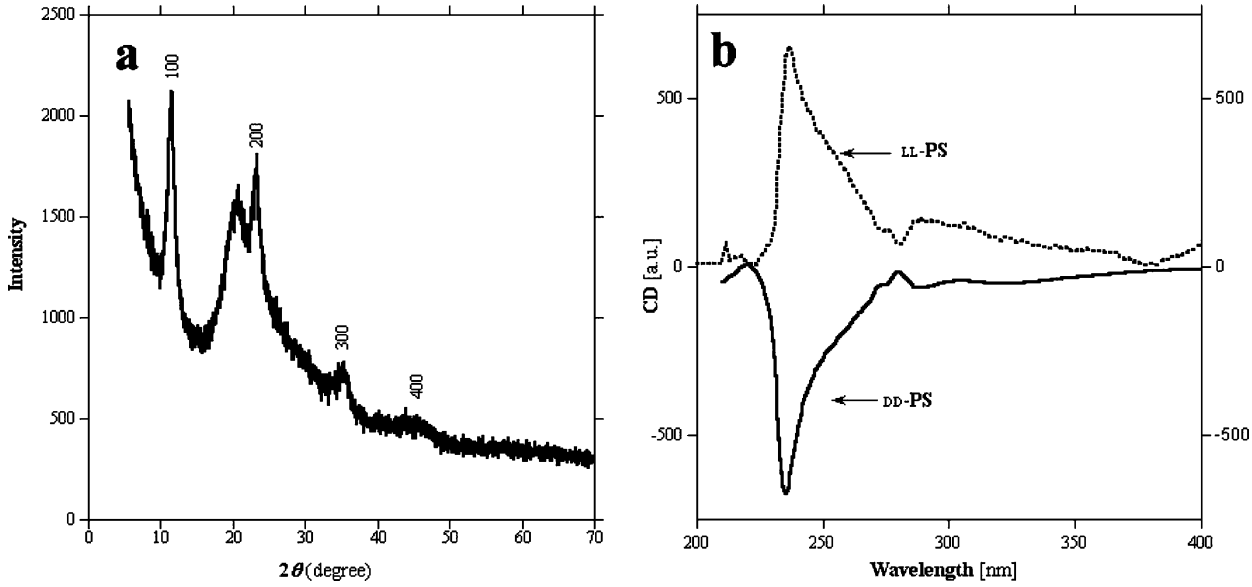

Figure 8. WAXRD pattern (a) of DD-**PS** and CD spectra (b) of LL-**PS** and DD-**PS** prepared under basic conditions.

obtained. The pore channels of the DD-**PS** are identified in Figure 6c and d. The nitrogen adsorption−desorption isotherm plot of the left-handed helical hybrid silica bundles is shown in Figure 7a. Both mesopore and macropore were identified. NLDFT pore-size distribution at the adsorption branch shows peaks from 2.0 to 2.7 nm (Figure 7b). The pore diameter is larger than that of 1,4-phenylene−silicas prepared under acidic conditions (Figure 3).

Figure 8a shows the WAXRD pattern of DD-**PS** prepared under basic conditions. It displays four peaks at medium diffraction angels at d = 7.6, 3.8, 2.5, and 1.9 Å. These diffraction peaks can be explained by a periodic structure with a spacing of 7.6 Å. This sample shows a greater degree of order than that prepared under acidic conditions. The average distance between two neighboring aromatic rings is 4.4 Å, which is longer than that of the sample prepared under acidic conditions. The pore channels do not seem to be periodic, no strong peaks were identified in SAXRD pattern (Supporting Information, Figure S5). The CD signs of LL-**PS** and DD-**PS** are shown in Figure 8b. For DD-**PS**, it shows two negative signs at 235 and 289 nm. On the contrary, LL-**PS** shows two positive signs at 238 and 289 nm. The CD signs should originate from the packing of the aromatic rings of hybrid silicas. On the first hand, the DD-**PS** shows two negative signs at 235 and 289 nm; however, gelator DD-**12PyBr** shows one positive CD sign at 200 nm. They show different CD signs. On the other hand, elemental analysis of the hybrid silica DD-**PS** shows 27.12 wt % of carbon, 5.18 wt % of hydrogen, and 0.0 wt % of nitrogen. The gelators should be totally removed by extracting. Therefore,

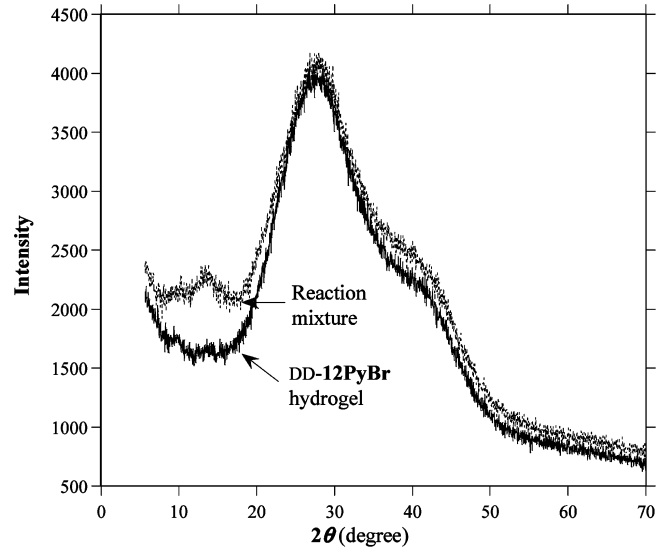

Figure 9. WAXRD patterns of the DD-**12PyBr** hydrogel and the reaction mixture under basic conditions.

the benzene rings of the hybrid silicas should be packing in helix. It has been reported previously that inner helical mesoporous silicas were prepared using the self-assemblies of LL-**12PyBr** as templates and TEOS as a silica source under basic conditions.[6a] Although straight mesoporous silica bundles were obtained, the mesopores are inner helical. For the hybrid silica bundles shown here, although most of them are also straight (Figure 6), the inner templates which can transfer the helicity to the packing of the aromatic rings are helical. This crystalline and helical packing on molecular level structure should find potential application in chiral separation and catalysis. For preliminary studying of the formation of this structure, WAXRD patterns of DD-**12PyBr** hydrogel and the reaction mixture after being left at room temperature for 48 h were taken (Figure 9). The packing of DD-**12PyBr** did not change during the sol−gel transcription process. The greater degree of order of aromatic rings should be formed after being left at 80 °C for four days.

(26) Snir, Y.; Kamien, R. D. *Science* **2005**, *307*, 1067.
(27) Han, Y.; Zhao, L.; Ying, J. Y. *Adv. Mater.* **2007**, *19*, 2454.
(28) Yang, S.; Zhao, L.; Yu, C.; Zhou, X.; Tang, J.; Yuan, P.; Chen, D.; Zhao, D. *J. Am. Chem. Soc.* **2006**, *128*, 10460.
(29) Tsuda, A.; Alam, Md. A.; Harada, T.; Yamaguchi, T.; Ishii, N.; Aida, T. *Angew. Chem., Int. Ed.* **2007**, *46*, 8198.
(30) Kim, W.-J.; Yang, S.-M. *Adv. Mater.* **2001**, *13*, 1191.
(31) Pokroy, B.; Kang, S. H.; Mahadevan, L.; Aizenberg, J. *Science* **2009**, *323*, 237.
(32) (a) Moreau, J. J. E.; Vellutini, L.; Wong Chi Man, M.; Bied, C. *Chem.−Eur. J.* **2003**, *9*, 1594. (b) Karatchevtseva, I.; Cassidy, D. J.; Wong Chi Man, M.; Mitchell, D. R. G.; Hanna, J. V.; Carcel, C.; Bied, C.; Moreau, J. J. E.; Bartlett, J. R. *Adv. Funct. Mater.* **2007**, *17*, 3926.

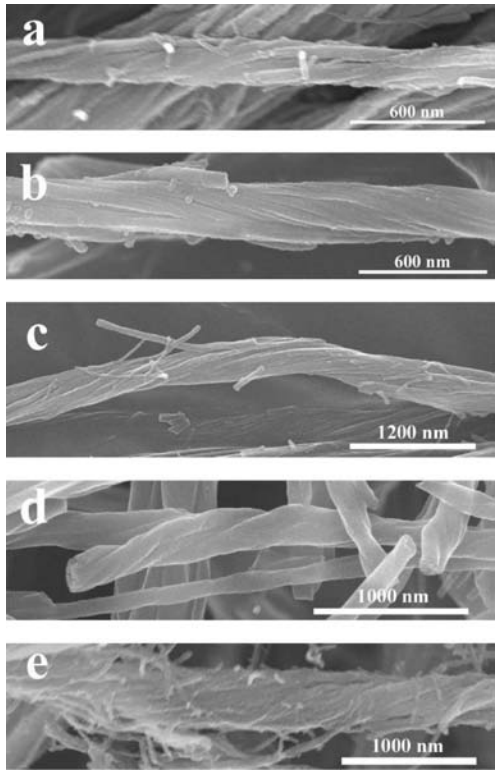

Figure 10. FESEM images of the left-handed helical silica bundles (a), right-handed helical silica bundles (b), the left-handed helical 1,3-phenylene−silica bundles (c), the left-handed helical ethene−silica bundles (d), and the left-handed helical ethane−silica bundles (e).

Multiple Helical Silica and Hybrid Silica Nanofibers under Acidic Conditions. As we show above, multiple helical nanofibers are likely formed under acidic conditions. Sol−gel transcription processes were carried out to prepare silicas and hybrid silicas. Left- and right-handed helical silica bundles were prepared using TEOS as precursor and the self-assemblies of LL-**12PyBr** and DD-**12PyBr** as templates, respectively (Figure 10a and b). For the hybrid silicas, all of them were prepared using the self-assemblies of LL-**12PyBr** as templates. Left-handed helical 1,3-phenylene−silica bundles, ethene−silica bundles, ethane−silica bundles were prepared using respectively **5**, **4**, and **3** as precursors. Generally, these bundles are hundreds of nanometers in diameter and hundreds of micrometers in length. The pore diameters are around 2.0 nm. For ethene−silica bundles, NLDFT pore-size distribution at adsorption branch shows a peak at 2.5 nm. Moreover, The BET surface area is 811 m^2/g (Supporting Information, Figure S6).

Conclusion

In summary, we successfully prepared helical silica and hybrid silica bundles via a sol−gel transcription method under acidic conditions. For 1,4-phenylene−silica bundles, they can be aligned during the sol−gel transcription process. Moreover, they show high thermostability. Crystalline and helix on a molecular level structure were obtained under basic conditions. They should be suitable for application in chiral separation and catalysis. Much work will be carried out in these fields.

Acknowledgment. This work was supported by the Program of Innovative Research Team of Soochow University, Natural Science Foundation of Jiangsu Province (No. BK2007047), and National Natural Science Foundation of China (No. 20871087).

Supporting Information Available: Experimental section; thermogravimetry analysis (TGA), graph of hybrid silica; FESEM and TEM images of calcined hybrid silicas; SAXRD pattern of DD-**PS** prepared under basic conditions; the nitrogen adsorption−desorption isotherm plot and NLDFT pore-size distribution at adsorption branch of ethene−silica bundles. These materials are available free of charge via the Internet at http://pubs.acs.org.

JA9001376